Dynamic Light Scattering Study of Salt Effect on Phase Behavior of Pig Vitreous Body and Its Microscopic Implication†

Masahiko Annaka,*,‡ Masahiro Okamoto,§ Toyoaki Matsuura,§ Yoshiaki Hara,§ and Sigeo Sasaki‡

Department of Chemistry, Faculty of Sciences, Kyushu University, 6-10-1, Hakozaki, Higashi-ku, Fukuoka 812-8581, Japan, and Department of Ophthalmology, Nara Medical University, 840 Shijyo-cho, Kashihara-shi, Nara 634-8522, Japan

Received: November 6, 2006; In Final Form: March 7, 2007

The salt effects on phase equilibrium and dynamical properties of pig vitreous body was studied by the macroscopic observation of the swelling behavior and dynamic light scattering under various conditions. It was found that the vitreous body collapses with maintaining the shape when the concentrations of salts (NaCl, $CaCl_2$, and $MgCl_2$) were changed. From the observations of the dynamics of light scattered by the pig vitreous body, intensity autocorrelation functions that revealed two diffusion coefficients, D_{fast} and D_{slow} were obtained. We developed the theory for describing the density fluctuation of the entities in the vitreous gel system with sodium hyaluronate filled in the meshes of the collagen fiber network. The dynamics of collagen and sodium hyaluronate explains two relaxation modes of the fluctuation. The diffusion coefficient of collagen obtained from D_{fast} and D_{slow} is very close to that in aqueous solution, which suggests the vitreous body is in the swollen state. Divergent behavior in the measured total scattered light intensities and diffusion coefficients upon varying the concentration of salt was observed. Namely, a slowing down of the dynamic modes accompanied by increased "static" scattered intensities was observed. This is indicative of the occurrence of a phase transition upon salt concentration.

1. Introduction

Biological polyelectrolyte gels consist of insoluble aggregates of molecules which collectively form structural fibrils and these fibrils, or their chemically bound side chains, have a net charge. These gels may be visualized as negatively charged fibrils immersed in aqueous solutions which include free diffusible ions.[1] A major property of gels, both synthetic and natural (biological) gels, is that they swell. All gels swell by the volume exclusion effect,[2] but gels which have a net nondiffusible electric charge on the macromolecules of their insoluble matrix swell in aqueous media not only through volume exclusion effects but also through internal electrostatic repulsion between neighboring matrix charges. The electrostatic repulsion between matrix charges is partly screened by mobile counterions in the aqueous medium penetrating the insoluble matrix.

The vitreous body is a tenuous gel that contains collagen and sodium hyaluronate.[3] The volume fraction of the polymer network is only about 1−2%, and the remaining is water. The vitreous body is located between the lens and the retina and comprises 80% of the overall volume of the eye. The functions of the vitreous body are supposed to keep the shape of the eyeball, to absorb the external mechanical shock, to maintain the homoeostasis of the eye, and to regulate the position of the lens. The appearance of fresh vitreous body is transparent, and hence, the vitreous body is considered a uniform tissue. Many studies performed to date have suggested that sodium hyaluronate, which has a coil shape, is uniformly distributed throughout the three-dimensional network of collagen fibers that form the triple helix in the vitreous body.[4] Essentially, no investigations on the structural, dynamics, and phase equilibrium properties of the vitreous body, however, have been performed to verify indisputably that the vitreous body is indeed a gel network. Some diseases affect changes in the complex structure of the vitreous body. The collapse of the vitreous body in the eye may cause many diseases such as posterior vitreous detachment, vitreous bleeding, and retinal detachment.[5,6]

Phase transition and critical phenomena observed in synthetic polymer gels are considered to be characteristics universal to all gels.[7,8] Regardless of their physicochemical composition, all polymer networks should then exhibit phase transitions and critical phenomena under appropriate conditions. A simple confirmation of their assertion was demonstrated by including phase transition in gels that were made up of cross-linked biopolymers.[9] The "bio-gels" were formed from artificially cross-linked biopolymers, such as DNA, agarose, and gelatin. However, there have been few studies detailing the phase transitions and critical phenomena of gels formed in nature. In investigations of the vitreous body, it had often been alluded to as a gel network. If indeed the vitreous body were a gel network, well-established theories would predict that the vitreous body should exhibit phase transition and critical phenomena in response to varied external conditions. The present research places the emphasis on the observation of the volume phase transition behaviors and the measurements of scattered light intensities and dynamics from pig vitreous body in vitro, subjected to the changes in the external conditions. It is natural to consider the collagen motion is coupled with the dynamics of sodium hyaluronate; therefore, we first develop the equation

† Part of the special issue "International Symposium on Polyelectrolytes (2006)".

* Corresponding author. Fax: +81-92-642-2594. E-mail: annaka-scc@mbox.nc.kyushu-u.ac.jp.

‡ Kyushu University.

§ Nara Medical University.

10.1021/jp067324f CCC: $37.00
Published on Web 05/31/2007

for the mode coupling of flexible sodium hyaluronate and the semirigid network of collagen. The unique physical properties of a gel arise from its structure. The gel is characterized by two kinds of bulk coefficients: (1) the elastic constants of the gel network and (2) the friction coefficients between the gel network and the fluid. We determine the friction coefficients between the vitreous gel network and gel fluid using a specially designed apparatus. Together with experimental and theoretical results of dynamic light scattering (DLS), we discuss the elastic properties of the pig vitreous body.

2. Theory for the Density Fluctuation of the Complex System of Polymers Filling in the Network Meshes

The situation that sodium hyaluronate fill in the meshes of collagen fiber network to prevent them from collapsing can be modeled as a complex system of polymers interacting with the network meshes. The DLS measures the time correlation of density fluctuation of the scattering entities, which are the segments of the sodium hyaluronate and the collagen mesh. The concentration fluctuation of the sodium hyaluronate segment, $\delta C_{HA}(\mathbf{r},t) = (C_{HA}(\mathbf{r},t) - C_{HA}^{0})$, where $C_{HA}(\mathbf{r},t)$ and C_{HA}^{0} respectively are the local and the averaged concentrations of the segment, can be described by the following diffusion equation.[10]

$$\frac{\partial \delta C_{HA}(\mathbf{r},t)}{\partial t} = D_{HA}\nabla^2 \delta C_{HA}(\mathbf{r},t) + L_{HA-Col} D_H \frac{C_{HA}^{0}}{C_{Col}^{0}} \nabla^2 \delta C_{Col}(\mathbf{r},t), \quad (1)$$

where D_{HA} and L_{HA-Col} respectively are a diffusion coefficient defined in the interparticle interaction free condition and a phenomenological coefficient, which is significant in the case that the acting force of the collagen matrix on the sodium hyaluronate is large. The subscripts, HA and Col, denote sodium hyaluronate and collagen, respectively. Here, C_{Col}^{0} and $\delta C_{Col}(\mathbf{r},t)$ respectively are the averaged concentration and the concentration fluctuation of the collagen segment. The collagen network can be regarded as an elastic body. According to the linear theory for the elastic body, a force balance among elastic and the external forces can be described by the following Newton equation.

$$\rho \frac{\partial^2}{\partial t^2}\mathbf{u} = \mu \vec{\nabla}^2 \mathbf{u} + \left(K + \frac{1}{3}\mu\right)\vec{\nabla}(\vec{\nabla}\cdot\mathbf{u}) - f\frac{\partial}{\partial t}\mathbf{u} + \mathbf{F}_{Col} \quad (2)$$

where ρ, $\mathbf{u}$, μ, K, f, and $\mathbf{F}_{Col}$ respectively are the density of the network, a displacement vector of the collagen segment, a shear modulus, a bulk modulus, a friction coefficient of a unit volume, and the force acted by the sodium hyaluronate, which is given by

$$\mathbf{F}_{Col} = -L_{Col-HA} T C_{Col}(\mathbf{r},t) \nabla \ln C_{HA}(\mathbf{r},t), \quad (3)$$

T is the Boltzmann temperature. Here, we use units where Boltzmann constant k_B is unity to use energy units for temperature. We should mention here the relation $f = C_{Col}{}^{0}\varsigma_{Col}$, where ς_{Col} is a friction coefficient of the collagen segment. The inertia term is negligibly small in the fluctuation; that is, $\rho\partial^2\mathbf{u}/\partial t^2 = 0$. Using eq 3 and the relationship $\vec{\nabla}\cdot\mathbf{u}(\mathbf{r}) = \delta C_{Col}(\mathbf{r},t)/C_{Col}^{0}$, we can rewrite eq 2 as

$$\frac{\partial \delta C_{Col}(\mathbf{r},t)}{\partial t} = D_S \nabla^2 \delta C_{Col}(\mathbf{r},t) + L_{Col-HA} D_{Col} \frac{C_{Col}{}^{0}}{C_H{}^{0}} \nabla^2 \delta C_{HA}(\mathrm{r},t), \quad (4)$$

where $D_S = (K + 4\mu/3)/f$, $D_{Col} = (T/f)C_{Col}^{0}$, and L_{Col-HA} is a phenomenological coefficient related to the acting force of sodium hyaluronate on the collagen matrix. From the solutions of eqs 1 and 4, we can obtain a double exponentially decaying function for the time correlation of the electric field of scattered light in Fourier space. A detail is described in Appendix.

3. Experimental Section

3.1. Materials. Pig vitreous bodies were isolated from sclera of the eyeball. The choroid membrane was also carefully removed by the standard method.[11] The samples were excised within 8 h after extraction of the eye at a local slaughterhouse. The approximate age of the pigs was 1 year. NaCl, $CaCl_2$, and $MgCl_2$ (Wako Pure Chemicals) are used as received.

3.2. Swelling Experiments. The effects of salts on the swelling ratio of the vitreous body were studied. The salt concentrations were changed from 1.0×10^{-7} to 1 mol/L using NaCl, $CaCl_2$, and $MgCl_2$. Since the size of the pig vitreous body was of the order of 4 cm^3 in volume, the time required to attain the equilibrium state was three weeks. Each solvent of sufficient volume was, therefore, changed every 2 days, and then the equilibrium/swelling ratio was determined. To avoid the growth of bacteria, we used the solvent containing 0.02% sodium azide especially for swelling experiments. This amount of sodium azide had no effect on the swelling ratio of the vitreous body. The swelling ratio of the vitreous body was determined by weighing in a gel in the equilibrium state. Both the weight of the sample at an equilibrium state in water, W_{water}, and the weight of the sample at an equilibrium state in an aqueous salt solution, W_{salt} (salt = NaCl, $CaCl_2$, $MgCl_2$), were measured. Then the swelling ratio was calculated from the ratio, W_{salt}/W_{water}. The solvent attached to the gel was carefully wiped to minimize the error.

3.3. Measurement of the Friction Coefficient. The principle of the measurement of the friction coefficient of a vitreous body is schematically shown in Figure 1. The apparatus was originally designed by Tokita and Tanaka, and they determined the friction coefficients of poly(acrylamide) gel and poly(*N*-isopropylacrylamide) gel accurately under various conditions.[12,13] A vitreous body of thickness d is fixed to the wall by silicon glue, and water is pushed through the vitreous body with a small pressure P. The average velocity of the water flow through the openings inside the vitreous gel, v, is determined by measuring the rate at which water flows out of the vitreous body in a steady state. The friction coefficient, f, is defined as

$$f = \frac{P}{d\cdot v}. \quad (5)$$

The chromatography column is used as a reservoir of water to generate the hydrostatic pressure. The range of the height of the water column can be changed from 20 to 60 cm, which corresponds to the pressure from 2×10^4 to 6×10^4 dyn/cm^2. The temperature of the sample is controlled within an accuracy of 0.1 °C. The apparatus is set on the vibration-free table to avoid any external mechanical disturbances. The rate of water flow through the gel was determined by measuring the movement of the water meniscus in a micropipette under a microscope.

3.4. Dynamic Light Scattering. DLS measurements on pig vitreous body were carried out using a DLS/SLS-5000 (ALV, Langen, Germany). A 22 mW He−Ne laser (Uniphase, U.S.A.) operating at 632.8 nm was used. In the DLS experiments, the full homodyne intensity autocorrelation function was determined with an ALV-5000 multiple-τ-digital correlator. Data were

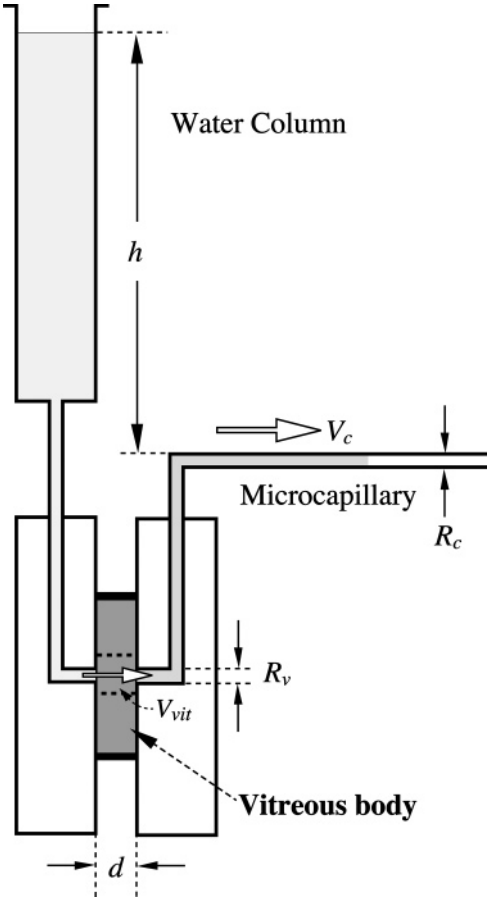

Figure 1. Schematic diagram of the apparatus for the measurement of the friction coefficient between the gel network and water. The sample mold is tightly held between two plexiglass plates. The velocity of the fluid flow in the micropipette is measured by a movable microscope with an accuracy of 0.001 mm.

obtained using a scattering angle ranging from 30 to 150° at a temperature of 37 °C unless stated.

The Siegert relation relates the normalized intensity autocorrelation function $g^{(2)}(q,t)$ to the normalized electric field autocorrelation function $g^{(1)}(q,t)$, assuming the scattered field has Gaussian statistics.

$$g^{(2)}(q,t) = 1 + B|g^{(1)}(q,t)|^2 \tag{6}$$

where B (≤ 1) is an instrumental parameter.

As we shall see later, a time autocorrelation function have a distinct double-exponential feature associated with cooperative diffusion ($\Gamma = Dq^2$, where Γ is the relaxation rate and D is the cooperative diffusion coefficient). This indicates the presence of two different diffusive modes within the gel. In this work, therefore, all of the correlation data were analyzed using the following relationship:

$$g^{(1)}(t) = A_{\text{fast}} \exp(-D_f q^2 t) + A_{\text{slow}} \exp(-D_s q^2 t) \tag{7}$$

with $A_{\text{fast}} + A_{\text{slow}} = 1$ where A_{fast} and A_{slow} are the amplitudes and D_f and D_s are the diffusion coefficients of the fast and slow components in the bimodal distribution, respectively, and $q = (4\pi n/\lambda) \sin(\theta/2)$ (n, refractive index; θ, scattering angle; and λ, wavelength of the incident beam) is the magnitude of the scattering vector.

4. Results and Discussions

4.1. Swelling Behavior. The swelling behavior of a gel is determined by the osmotic pressure of the gel. The osmotic pressure of the gel consists of four contributions, that is, the rubber elasticity of the polymer network, the effects of the counterion of the ionic group on the polymer network, the interaction free energy between the polymer and the solvent, and the mixing entropy. The balance of these four factors determines the equilibrium swelling ratio of the gel.[7] The vitreous body is a typical biological gel that consists of collagen and sodium hyaluronate. The collagen is a main protein component of the vitreous body.[3] Hyaluronic acid is a typical acidic mucopolysaccharide carrying carboxyl groups as the ionic side chain. These components form a complex in the vitreous gel and built-up the three-dimensional polymer networks of the gel. The vitreous body is, therefore, one of the multicomponent ionic gels.

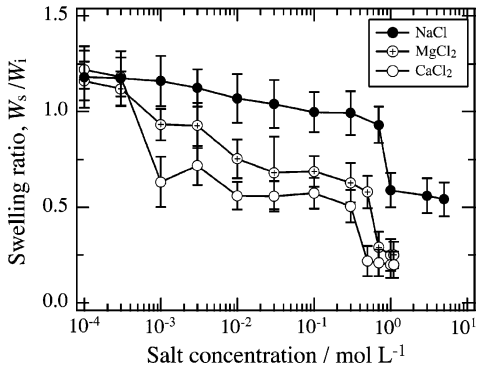

Figure 2. Swelling ratio of pig vitreous body in different concentrations of NaCl, $MgCl_2$, and $CaCl_2$ aqueous solutions at 37 °C ($n = 5$ for each concentration).

Figure 2 shows the swelling ratios of the vitreous body as a function of the concentrations of aqueous solutions of NaCl, $CaCl_2$, and $MgCl_2$ at 37 °C. A marked decrease in swelling ratio is observed when the salt concentration in the external solution is increased. This is in accordance with the Donnan equilibrium theory, which predicts that the difference in ionic concentration between the inside and the outside of a gel decreases when the concentration of salt in the surrounding liquid is increased. No hysteresis was observed in the swelling curves.

The osmotic pressure, Π, of a charged gel is given by[15,16]

$$\Pi = \Pi_{\text{mix}} + \Pi_{\text{elastic}} + \Pi_{\text{ion}} = -\frac{\Delta\mu}{V_s} \tag{8}$$

where V_s is the molar volume of the solvent and $\Delta\mu$ is the chemical potential change caused by gel swelling. Π_{mix}, Π_{elastic}, and Π_{ion} are the contributions to the osmotic pressure due to polymer−solvent mixing, polymer chain elasticity, and the Donnan potential, respectively. In the context of the conventional theory of swelling,[15] Π_{mix} and Π_{elastic} are functions of the polymer volume fraction, ϕ, and are given by

$$\Pi_{\text{mix}} = -\frac{RT}{\upsilon}[\phi + \ln(1-\phi) + \chi\phi^2] \tag{9}$$

and

$$\Pi_{\text{elastic}} = \nu_e RT \frac{1}{2}\left[\left(\frac{\phi}{\phi_0}\right) - \left(\frac{\phi}{\phi_0}\right)^{1/3}\right] \tag{10}$$

where R is the gas constant, υ is the molar volume of the lattice (i.e., the molar volume of the segment), χ is the Flory−Huggins interaction parameter, ν_e is the number of effective chains contributing to the elasticity per unit volume, and ϕ_0 is the polymer volume fraction at the reference state.

Because of its network structure, the gel acts as if it provides its own semipermiable membrane. To allow for changes in swelling caused by altering the concentration of salts outside the gel, it is necessary to treat the ionic term, Π_{ion}, as the effective difference in chemical potential of the solvent due to mobile ions inside the gel. The osmotic pressure generated by the Donnan potential is then given by[15]

$$\Pi_{ion} = -\frac{\Delta\mu}{V_s} \approx RT\Delta C_{mobile} \tag{11}$$

The effective osmolarity of the mobile ions, ΔC_{mobile} (i.e., the concentration difference of mobile ions between the inside and the outside of the gel), is given by

$$\Delta C_{mobile} = (C_+ + C_-) - (C'_+ + C'_-) \tag{12}$$

where C_+ and C_-, and C'_+ and C'_- are the concentrations of positive and negative mobile ions inside and outside the gel, respectively. The ion concentrations are determined by the Donnan equilibrium,[15] which for anionic polymers in 1:1 and 2:1 electrolytes are described by the following equations:

$$z_+C_+ = z_-C_- + z_pC_p \qquad \text{(inside the gel)} \tag{13-1}$$

$$z_+C'_+ = z_-C'_- \qquad \text{(outside the gel)} \tag{13-2}$$

$$\gamma_\pm^2\, C_-^{z_-}\, C_-^{z_+} = \gamma'^{\,2}_\pm C'^{\,z_-}_+ C'^{\,z_+}_-, \tag{13-3}$$

where C_+ and C_- are the absolute values of the valences of the mobile ions, z_p is the number of noncondensed charges per monomer residue, C_p is the concentration of polymer in the gel expressed as the molar concentration of monomer residues, and $\gamma_\pm$ and $\gamma'_\pm$ are the mean activity coefficients of the salt inside and outside the gel, respectively. The fraction of noncondensed ions per monomer residue, z_p, can be calculated from the Manning theory of counterion condensation. The chain may be characterized by a dimensionless parameter ξ,

$$\xi = \frac{e^2Q}{Dk_BTL} \tag{14}$$

where e is the electron charge, Q is the number of (electron) charges in length L, D is the bulk solvent dielectric constant, k_B is the Boltzmann constant, and T is the absolute temperature. For monovalent counterions, the value $\xi = 1$ regarded as a critical value, above which counterion condensation occurs in some fraction near the polyion and below which the polyion, may be regarded as fully ionized.[17] The value of ξ for the hyaluronate polyion was taken to be 0.70,[18,19] which is below the critical value. Here, we assume that the polymer is fully ionized in the Debye−Hückel sense.

By numerical analysis of the equations which determine the degree of swelling of a gel (eqs 9 and 11), the ionic term is the significant term contributing to the swelling pressure of the vitreous gel as indicated in Figure 3a. This behavior, therefore, can be explained on the basis of the Donnan-equilibria argument. According to eq 11, the chemical potential difference due to the Donnan equilibrium is proportional to the concentration difference between mobile ions inside and outside the gel, ΔC_{mobile}. Figure 3b shows the calculated concentration difference of ions for 1:1 (NaCl) and 2:1 ($CaCl_2$ and $MgCl_2$) electrolytes. This can be compared to the swelling curves for the same electrolytes. The good correlation, which is observed between observed and calculated swelling curves, indicates that the

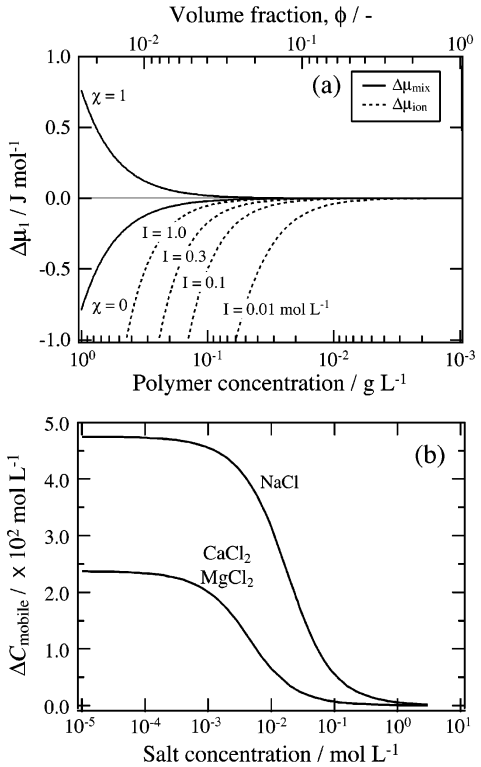

Figure 3. (a) Numerical evaluation of the terms contribution to change in chemical potential for the solvent ($\Delta\mu_1$) in a sodium hyarulonate as a function of polymer concentration and of volume fraction of polymer: dotted line, ionic term (ideal Donnan term); solid line, mixing term. Specific volume of polymer is assumed to be 0.5 mL/g. (b) Difference in ion concentration between the inside and the outside of a vitreous gel (effective osmolarity in the gel) as a function of electrolyte concentration calculated using the theory of ideal Donnan equilibrium for a 1:1 (NaCl) and 2:1 ($MgCl_2$ and $CaCl_2$) electrolyte. It is assumed that no counterion condensation takes place. Polymer concentration, $C_{polymer}$ is assumed to be 10 g/L.

Donnan equilibrium is the main factor determining the swelling behavior of the gel.

The vitreous gel swells in $10^{-7}-10^{-4}$ mol/L of the salt solution because of the charge repulsion force of the carboxylate group on hyaluronic acid, resulting in expansion of the gel networks. When the salt concentration of the external solution increased from $10^{-4}-10^{-3}$ mol/L, the negative charges in hyaluronic acid were neutralized by the cations, and the swelling ratio rapidly decreased; that is, the gel shows a de-swelling behavior. Almost all of the negative charges on the polymer chains were neutralized by the external cations in this concentration range. This results from the Donnan effect. However, the salt concentration further increased over 10^{-3} mol/L; the vitreous gel became a nonionic-type hydrogel, and therefore the swelling curve reflected nearly a horizontal line in the range of $10^{-3}-10^{-1}$ mol/L. When the salt concentration was raised to 1 mol/L, the salting-out effect was enhanced because of the high external ionic concentration, and the swelling ratio of the vitreous gel sharply decreased.

4.2. Friction Coefficient. The velocity of the water in the micropipette at the stationary state, V_c, is obtained by measuring the shift of the water meniscus for a given period of time using a movable microscope with an accuracy of 0.001 mm. The velocity thus obtained is plotted as a function of the pressure in Figure 4. At relatively high pressures, the water flow in the vitreous body is high. Presumably, the network structure of the vitreous body is broken under high pressure; therefore, we chose five points measured at lower pressure to calculate the friction

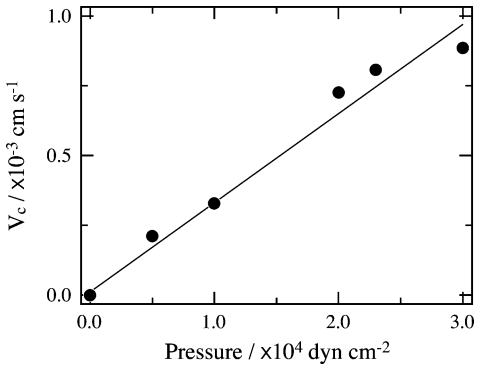

Figure 4. Velocity of water in the micropipette is plotted as a function of the water pressure. The solid line in this figure is obtained by the least-square fit.

coefficients. The relationship between the applied pressure and the velocity is linear at lower pressures as predicted. The friction coefficient between vitreous body and water, $f = 6.4 \times 10^9$ dyn·s/cm^4, was obtained from the slope of the straight line in Figure 4 using the following equation:

$$f = \left(\frac{dV_C}{dp}\right)^{-1} \cdot \frac{1}{d} \cdot \left(\frac{R_V}{R_C}\right)^2, \tag{15}$$

where, $dV_C/dp = 3.1 \times 10^{-8}$ cm^3/dyn·s is determined from the slope of the straight line as given in Figure 4. The thickness of the sample, d, is $d = 0.5$ cm. The factor $(R_V/R_C)^2$ is the ratio of the area of the micropipette of radius $R_c = 3.4 \times 10^{-2}$ cm and the area of the hole in the vitreous body with radius $R_v = 3.3 \times 10^{-1}$ cm, which is necessary to convert V_c to V_{vit}. The value of f measured here is from the total water flow along the orbital axis in the vitreous body. More precise measurements at different positions are needed, but it is very difficult to measure water flow in a high-water-content vitreous body without destruction of its network structure. Therefore, we use this friction coefficient in the following discussions.

4.3. Dynamic Light Scattering. Pig vitreous bodies were investigated by DLS in aqueous solutions of NaCl and $CaCl_2$. Intensity correlation functions were recorded at five different scattering angles between 30 and 150°. For each scattering angle, the measurements were repeated five times, and the values for relaxation times given below are averaged of these five measurements.

Figure 5 shows the scattering angle dependence of (a) the normalized electric field autocorrelation function, $g^{(1)}(\tau)$ versus tq^2, and (b) the decay rate distribution functions, $G(\Gamma)$ versus $\Gamma^{-1}q^2$ for the pig vitreous body immersed in 0.16 mol/L aqueous solutions of NaCl (saline). For all scattering angles, two significant contributions are resolved as shown in Figure 5b, and all of the distribution functions can be roughly superimposed to each other. We observed some deviation which is, however, close to a limit of the experimental error. This indicates that the observed two modes are diffusive. For a diffusive mode, one expects that Γ is proportional to q^2. For all scattering angles, the Γq^{-2} for both fast and slow modes are almost q independent as shown in Figure 6. This indicates that the observed two modes are diffusive. It should be mentioned that the apparent q^2 dependence of the Γq^{-2} is within experimental error. The essential parameters for the diffusion coefficients D_{fast} and D_{slow} that represent the two apparent, collective diffusion motions of the vitreous gel, designated as fast and slow motions, respectively, were derived. The results of the fits yielded for $D_{fast} = (5.9 \pm 0.83) \times 10^{-12}$ m^2/s and $D_{slow} = (1.9 \pm 0.78) \times 10^{-13}$ m^2/s for vitreous gel in saline (data shown in Figure 6).

Other significant parameters of the fit include the relative contributions of the fast and slow components to overall dynamic scattered light intensity, I_D, designated as $\%A_{fast}$ and $\%A_{slow}$, respectively, where $\%A_{fast} = 100 \times A_{fast}/(A_{fast} + A_{slow})$. The static $\%I_S$ and dynamic $\%I_D$ components of scattered light intensities, where $\%I_D = 100 \times I_D/(I_S + I_D)$, to the total scattered light intensity I_{total} observed at a particular wave vector, were also determined. The temporal fluctuations of the scattered light intensity $I(t)$ were analyzed in terms of intensity autocorrelation functions[20]

$$G^{(2)}(\tau) = \langle I(t) \cdot I(t+\tau) \rangle \tag{16}$$

where $\langle\ \rangle$ stands for the time average over t. The rate of the fluctuations of the scattered light intensity, that represent the density fluctuations of the vitreous gel, is proportional to the rate of local swelling and shrinking of the gel via molecular Brownian motions. There are also permanent and static inhomogeneities within the vitreous that also contribute to light scattering. The static inhomogeneities are characteristic of polymer gels and arise from topological constrains of the network chain molecules. The light intensity scattered by these inhomogeneities does not fluctuate with time. The scattered light intensity is, thus, the superposition of contributions from scattering elements that are static from those that dynamically fluctuate:[21]

$$I(t) = I_S + I_D(t) \tag{17}$$

In DLS, the time correlation of the intensity of scattered light is recorded. Assuming the Gaussian nature of the scattered light photons, the correlation function of the intensity of scattered light is rewritten in terms of the autocorrelation function $G^{(1)}(\tau)$ of the scattered electric field $E(t)$, that is related to the scattered light intensity: $I(t) = E(t)E^*(t)$,[20]

$$G^{(1)}(\tau) \equiv \frac{\langle E(t) \cdot E^*(t+\tau) \rangle}{\langle E(t) \cdot E^*(t) \rangle} \tag{18}$$

Then $G^{(2)}(\tau)$ is written as

$$G^{(2)}(\tau) = (I_S + I_D)^2 + A\{I_D^2 \cdot G^{(1)2}(\tau) + 2I_S \cdot I_D G^{(1)}(\tau)\} \tag{19}$$

where A is the efficiency parameter of the apparatus, which is uniquely determined by the optical configuration of the setup, the value I, and the average intensities scattered by the gel fluctuations and the static inhomogeneities.[21] On the basis of eqs 16−19, for the data in Figure 5, $\%A_{slow} \approx 61 \pm 5$ and $\%I_D \approx 22 \pm 3$ for vitreous gel in saline at 37 °C.

5. Discussion

The vitreous body can be regarded as a gel composed of the highly flexible sodium hyaluronate polymers. The fluid gel is interwoven by a semirigid network of collagen threads which serve the mechanical stabilization of the body. As mentioned in the theoretical section, the DLS measures the time correlation of density fluctuation of the scattering entities, which are segments of the hyaluronate polymers and the collagen mesh. The vitreous body is found to show two different diffusion coefficient modes, one relatively fast and the other a relatively slow mode. This may be due to the complex structure of the vitreous body, in which the highly flexible sodium hyaluronate is interwoven by semirigid collagen threads.[9] In this case, it is natural to consider the coupling of the collagen motion with the dynamics of sodium hyaluronate which can explain the fast

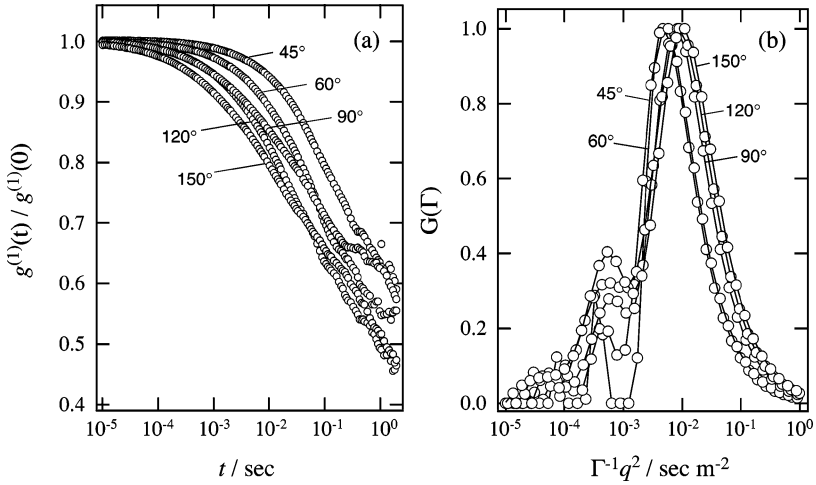

Figure 5. (a) Scattering angle dependence of normalized electric field autocorrelation function, $g^{(1)}(\tau)/g^{(1)}(0)$ vs t, and (b) the relaxation time distribution for the pig vitreous body in saline at 37 °C.

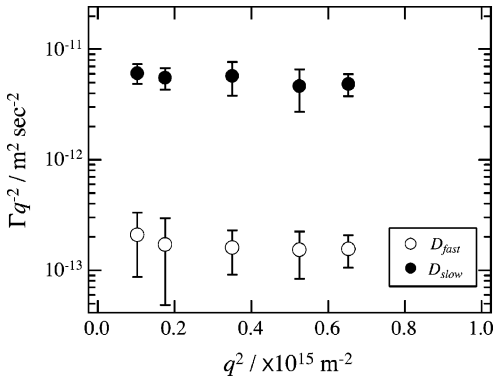

Figure 6. q^2 dependence of the Γq^{-2} for the pig vitreous body in saline at 37 °C.

mode. According to eqs A4 and A8 in Appendix, $D_{\text{fast}}(=\lambda_1)$ and $D_{\text{slow}}(=\lambda_2)$ are given by

$$D_{\text{fast}} = D_{\text{HA}} - \Delta D \quad \text{and} \quad D_{\text{slow}} = D_{\text{S}} + \Delta D \; (D_{\text{HA}} > D_{\text{S}}), \tag{20}$$

and

$$D_{\text{fast}} = D_{\text{S}} - \Delta D \quad \text{and} \quad D_{\text{slow}} = D_{\text{HA}} + \Delta D \; (D_{\text{HA}} < D_{\text{S}}), \tag{21}$$

Takahashi et al.[22] measured the diffusion coefficient of sodium hyaluronate diluted in the 0.2 M NaCl aqueous solution, molecular weight of which is similar to that ($M_{\text{w}} \sim 1.4 \times 10^6$) in the pig vitreous body by DLS, and found to be $D_{\text{HA}} \approx 2.4 \times 10^{-12}$ m^2/s. Using this result, we evaluated the values of D_{S}, ΔD, and $D_{\text{Col}}L_{\text{Col-HA}}L_{\text{HA-Col}}$ from the obtained D_{fast} and D_{slow} values, and they were found to be $D_{\text{S}} = 3.7 \times 10^{-12}$ m^2/s, $\Delta D = -2.2 \times 10^{-12}$ m^2/s, and $D_{\text{Col}}\, L_{\text{Col-HA}}\, L_{\text{HA-Col}} = 11 \times 10^{-12}$ m^2/s. It should be mentioned that the value of $D_{\text{Col}}L_{\text{Col-HA}}L_{\text{HA-Col}}$ is very close to the reported diffusion constant of collagen with a contour length of 280 nm in 0.1 N HCl aqueous solution ($D_{\text{Col}} \sim 9 \times 10^{-12}$ m^2/s).[23] It is plausible that the $L_{\text{Col-HA}}L_{\text{HA-Col}}$ value for the collagen strongly coupled to sodium hyaluronate in the vitreous body is 1 order of magnitude. It can be inferred, therefore, that the collective diffusion coefficient of collagen in the vitreous body is very close to that in the aqueous solution. This can be realized in the highly swollen vitreous body which has enough space for the polymer segments to move freely.

The elastic moduli, M ($= K + 4\mu/3$), estimated from the D_{S} and f values ($f \approx 6.4 \times 10^9$ dyn·s/cm^4) using eq 3 is 240 Ps. The intraocular pressure is created by the continual renewal of fluids within the interior of the eye, and is known to be within the range of 1300−2600 Ps (≈10−20 mmHg) under normal physiological conditions. It is clinically known that the intraocular pressure is reduced to less than 670 Ps (≈5 mmHg) by artificially blocking the production of aqueous humor. In this case, only the elastic modulus of the gel network is considered to contribute to the intraocular pressure; therefore, our experimental results are consistent with the clinical observation.

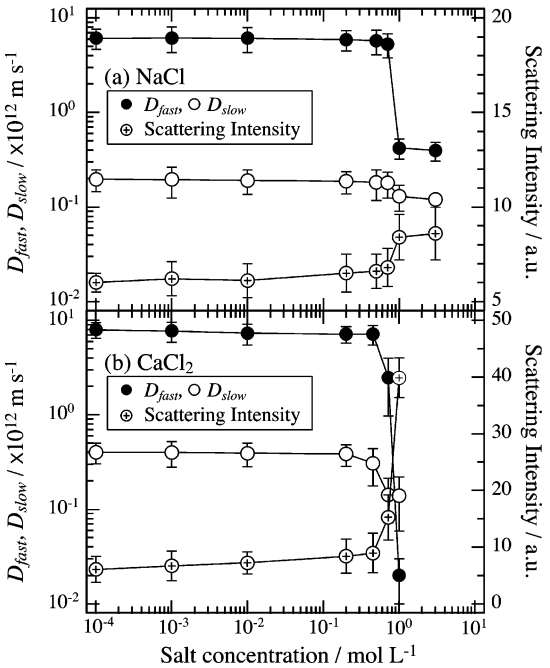

Figure 7. Diffusion coefficients, D_{fast} (○) and D_{slow} (●), and scattered light intensity (⊕) as a function of (a) NaCl and (b) $CaCl_2$ concentrations at 37 °C ($n = 5$ for each concentration). The solid lines are a guide for the eyes.

The dynamics of vitreous gels were observed with respect to externally increased NaCl and $CaCl_2$ concentrations. Figure 7 shows the averaged fast and slow diffusion coefficients, D_{fast} and D_{slow}, and the measured scattered light intensity I_{total} in aqueous solutions of (a) NaCl and (b) $CaCl_2$ in the concentration range between 1.0×10^{-4} and 3.0 mol/L (1.0 mol/L for $CaCl_2$). The diffusion coefficients gradually decreased with the concentration of salt. It is remarkable that the diffusion coefficient diminished at 1 mol/L of $CaCl_2$. It is worthy to mention that

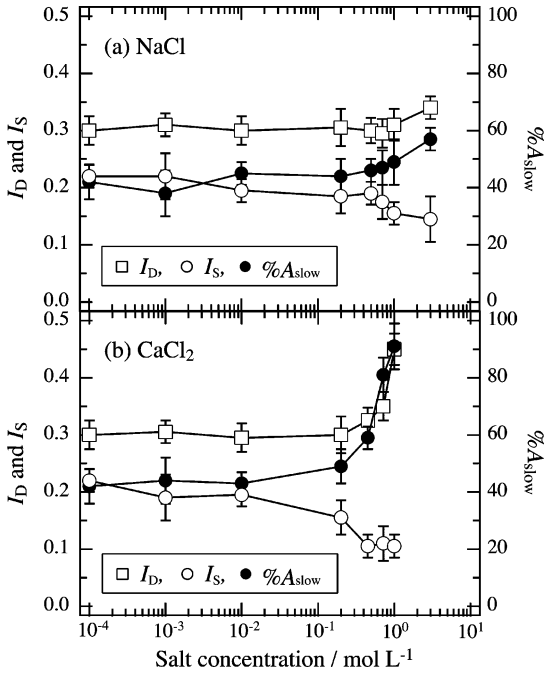

Figure 8. Changes in the static and dynamic components, I_S (□) and I_D (○), contributed to the total scattered intensity I_{total} (●) as a function of (a) NaCl and (b) $CaCl_2$ concentrations at 37 °C ($n = 5$ for each concentration). The corresponding contribution of the "slow" scatterer $\%A_s$ to the overall increase in I_D is also shown ($n = 5$ for each concentration). The solid lines are a guide for the eyes.

the vitreous body became slightly opaque as a threshold for $CaCl_2$ concentration was approached in the range of 1 mol/L.

Parallel to the diminishment of the diffusion coefficients, the measured intensity I_{total} from the vitreous body in the $CaCl_2$ solution observed at 90° increased and appeared to diverge as the concentration approached the critical threshold, 1 mol/L (Figure 8). No remarkable change was observed for I_{total} from the vitreous body in the NaCl solution. The changes in I_{total} can be attributed to the increased compressibility of the vitreous gel as it approached the critical point of concentration. The divergent behavior in the observed diffusion coefficients and total scattered light intensities is indicative of the occurrence of a phase transition upon the calcium ion concentration. These changes were reversible.

Under the condition of increased $CaCl_2$ concentration, the vitreous body approached a critical point where it became opaque. Critical opalescence occurs as a result of large-scale temporal fluctuations in the local densities of the collagen gel, where regions of high and low collagen densities form. Therefore, as a phase transition is approached, the magnitude of intensity fluctuations is increased while they become slowed down. This behavior was readily evidenced by a divergent behavior in the observed scattered light intensities (I_{total}) and diffusion coefficients (D_{fast} and D_{slow}). Moreover, the dramatic increase in the observed scattered light intensities I_{total} is associated directly with an increase in the dynamic component of the scattered light I_D rather than the static component I_S (Figure 8). The primary contributor to the increase in I_D is the "slow" mode, where an increase in $\%A_s$ is also observed as the calcium concentration was increased (Figure 8). This behavior is indicative of a gel undergoing a phase transition.

6. Conclusion

DLS spectroscopy was applied to investigate the structural and dynamical properties of pig vitreous body. From the observations of the dynamics of scattered light scattered by the pig vitreous body, two different diffusive modes, one relatively fast and the other relatively slow, were observed. We developed the coupling theory in a vitreous gel system describing the coupling of the collagen motion with the dynamics of sodium hyaluronate under the assumption that sodium hyaluronate was filled in the meshes of the collagen fiber network. The calculated value of the diffusion coefficient of collagen is very close to that in aqueous solution, which suggests the vitreous body is in the swollen state and provides the validity of our model. The diffusion coefficients from the intensity correlation function decreased with the concentration of $CaCl_2$ and diminished at 1 mol/L. Parallel to the diminishment of the diffusion coefficients, the measured intensity increased and appeared to diverge as the concentration approached 1 mol/L. The divergent behavior in the observed diffusion coefficients and total scattered light intensities is indicative of the occurrence of a phase transition upon the calcium ion concentration. No remarkable changes are observed with increasing NaCl concentration. In the quest for the principle cause behind diseases of the vitreous body, a more precise study, however, must be needed to reveal the structural and dynamical properties of the vitreous body at a molecular level. This study represents new structural and dynamic properties of the vitreous body. The simple consideration presented here may be helpful toward the understanding of physicochemical aspects of diseases. To develop a more thorough understanding of the vitreous gel, however, much more conclusive investigations are warranted under various conditions, which is the subject of future studies.

Acknowledgment. The work was partly supported by a Grant-in-Aid for Scientific Research from the Ministry of Education, Science, Sports and Culture (for M.A., 17350060). M.A. and T.M. acknowledge HOYA Corporation and Iketani Science and Technology Foundation for financial support.

Appendix

Mode Coupling of Flexible Sodium Hyaluronate and the Semirigid Network of Collagen. Equations 1 and 4 can be rewritten in the form of Fourier transform of the concentrations as:

$$\frac{\partial C_{HA}(q,t)}{\partial t} = -q^2\left\{D_{HA}C_{HA}(q,t) + L_{HA-Col}D_{HA}\frac{C_{HA}^{\ 0}}{C_{Col}^{\ 0}}C_{Col}(q,t)\right\} \quad \text{(A1)}$$

$$\frac{\partial C_{Col}(q,t)}{\partial t} = -q^2\left\{D_S C_{Col}(q,t) + L_{Col-HA}D_{Col}\frac{C_{Col}^{\ 0}}{C_{HA}^{\ 0}}C_{HA}(q,t)\right\} \quad \text{(A2)}$$

where

$$\delta C_{HA}(\mathbf{r},t) = \left(\frac{1}{2\pi}\right)^3 \int\int\int d\mathbf{r}^3 C_{HA}(\mathbf{q},t)\exp(i\mathbf{q}\cdot\mathbf{r})$$

and

$$\delta C_{Col}(\mathbf{r},t) = \left(\frac{1}{2\pi}\right)^3 \int\int\int d\mathbf{r}^3 C_{Col}(\mathbf{q},t)\exp(i\mathbf{q}\cdot\mathbf{r})$$

Equations 5 and 6 can be converted into matrix form as

$$\frac{\partial}{\partial t}\mathbf{C}(\mathbf{q}) = -q^2\tilde{A}\mathbf{C}(\mathbf{q}), \quad \text{(A3)}$$

where

$$\mathbf{C}(\mathbf{q}) = \begin{pmatrix} C_{HA}(\mathbf{q},t) \\ C_{Col}(\mathbf{q},t) \end{pmatrix} \quad \text{and} \quad \tilde{A} = \begin{pmatrix} D_{HA} & L_{HA-Col} D_{HA} \dfrac{C_{HA}^{\ 0}}{C_{Col}^{\ 0}} \\ L_{Col-H} D_{Col} \dfrac{C_{Col}^{\ 0}}{C_{HA}^{\ 0}} & D_S \end{pmatrix}$$

The solution of eq A3 is given as

$$\begin{pmatrix} C_{HA}(\mathbf{q},t) \\ C_{Col}(\mathbf{q},t) \end{pmatrix} = B(\mathbf{q}) \begin{pmatrix} D_1(\mathbf{q}) \exp(-q^2\lambda_1 t) \\ D_2(\mathbf{q}) \exp(-q^2\lambda_2 t) \end{pmatrix},$$

where

$$\tilde{B}^{-1}(\mathbf{q})\tilde{A}(\mathbf{q})\tilde{B}(\mathbf{q}) = \begin{pmatrix} \lambda_1 & 0 \\ 0 & \lambda_2 \end{pmatrix},$$

with

$$2\lambda_{1\text{ or }2} = D_{HA} + D_S \pm [(D_{HA} - D_S)^2 + 4D_{HA}L_{Col-HA}D_{Col}L_{HA-Col}]^{1/2} \quad (\lambda_1 \geq \lambda_2) \quad \text{(A4)}$$

and

$$\tilde{B} \approx \frac{1}{\sqrt{D_{HA}L_{Col-HA}D_{Col}L_{HA-Col} + \Delta D^2}} \begin{pmatrix} L_{Col-HA}D_{Col}\dfrac{C_{Col}^{\ 0}}{C_{HA}^{\ 0}} & \Delta D \\ -\Delta D & L_{HA-Col}D_{HA}\dfrac{C^0_{HA}}{C^0_{Col}} \end{pmatrix}$$

$$\tilde{B}^{-1} \approx \frac{1}{\sqrt{D_{HA}L_{Col-HA}D_{Col}L_{HA-Col} + \Delta D^2}} \begin{pmatrix} L_{HA-Col}D_{H}\dfrac{C_{HA}^{\ 0}}{C_{Col}^{\ 0}} & -\Delta D \\ \Delta D & L_{Col-HA}D_{Col}\dfrac{C_{Col}^{\ 0}}{C_{HA}^{\ 0}} \end{pmatrix}$$

$$\Delta D = \frac{|D_S - D_{HA}|}{2}\{1 - \sqrt{1 + 4D_{HA}L_{Col-HA}D_{Col}L_{HA-Col}(D_{HA} - D_S)^{-2}}\}, \quad \text{(A5)}$$

Thus, the concentration fluctuations can be given by

$$C_{HA}(\mathbf{q},t) \propto L_{Col-HA}D_{Col}\frac{C_{Col}^{\ 0}}{C_{HA}^{\ 0}} \exp(-q^2\lambda_1 t) + \Delta D \exp(-q^2\lambda_2 t) \quad \text{(A6)}$$

$$C_{Col}(\mathbf{q},t) \propto -\Delta D \exp(-q^2\lambda_1 t) + L_{HA-Col}D_{HA}\frac{C_{HA}^{\ 0}}{C_{Col}^{\ 0}} \exp(-q^2\lambda_2 t), \quad \text{(A7)}$$

Finally, eq A7 yields a double exponentially decaying function for the time correlation of the electric field of scattering light as follows:

$$g^{(1)}(q,\tau) \propto A_{fast} \exp(-q^2\lambda_1 t) + A_{slow} \exp(-q^2\lambda_2 t) \quad \text{(A8)}$$

where A_{fast} and A_{slow} are constants.

References and Notes

(1) Elliotto, G. F.; Hodoson, S. A. *Rep. Prog. Phys*. **1998**, *61*, 1325.
(2) Flory, P. J. *Statistical Mechanics of Chain Molecules;* Oxford University Press: New York, 1989.
(3) Berman, E. R.; Voaden, M. In *Biochemistry of the Eye;* Smelser, G. K., Ed.; Academic Press: London, 1970; p 373.
(4) Balazs E. A. In *New and Controversial Aspects of Retinal Detachment;* McPherson, A., Ed.; Academic Press: Philadelphia, 1968; Vol. 1, p 3.
(5) William S. T. T. *Am Acad. Opthalmol. Otolaryngol*. **1968**, *72*, 217.
(6) Norman, S. J. *Arch. Ophthalmol*. **1968**, *79*, 568.
(7) Tanaka, T. *Phys. Rev. Lett.* **1978**, *40*, 820.
(8) Shibayama M.; Tanaka, T. *Adv. Polym. Sci*. **1993**, *109*, 1.
(9) Amiya T.; Tanaka, T. *Macromolecules* **1987**, *20*, 1162.
(10) Sasaki, S.; Schipper, F. M. J. *J. Chem. Phys*. **2001**, *115*, 4349.
(11) Worst, J. G. F.; Los, L. I. *Cisternal Anatomy of the Vitreous;* Kugler Publications: Amsterdam, The Netherlands, 1995; p 1.
(12) Tokita, M.; Tanaka, T. *J. Chem. Phys.* **1991**, *95*, 4613.
(13) Tokita, M.; Tanaka, T. *Science*. **1991**, *253*, 1121.
(14) Tanaka, T.; Hocker, L. O.; Benedek, G. B. *J. Chem. Phys.* **1973**, *59*, 5151.
(15) Tanaka, T.; Fillmore, D.; Nishio, I.; Sun, S.-T.; Shah. A.; Swislow, G. *Phys. Rev. Lett.* **1980**, *45*, 1636.
(16) Flory, P. J. In *Principle of Polymer Chemistry;* Cornell University Press: Ithaca, NY, 1953; pp 541−593.
(17) Manning, G. S. *J. Chem. Phys*. **1969**, *51*, 924.
(18) Cleland, R. L.; Wang, J. L.; Detweiler, D. M. *Macromolecules* **1982**, *15*, 386.
(19) Cleland, R. L. *Macromolecules* **1982**, *15*, 382.
(20) Ohmine, I.; Tanaka, T. *J. Chem. Phys*. **1982**, *77*, 5725.
(21) Ricka, J.; Tanaka, T. *Macromolecules* **1984**, *17*, 2916.
(22) Creighton, T. E. *Proteins, Structure and Molecular Properties;* Freeman: New York, 1984.
(23) Berne, B.; J. Pecora, R. *Dynamic Light Scattering;* Plenum Press: New York, 1976.
(24) Peeterman, J.; Nishio, I.; Onishi, S.; Tanaka, T. *Proc. Natl. Acad. Sci. U.S.A.* **1986**, *83*, 352.
(25) Takahashi, R.; Kubota, K.; Kawada, M.; Okamoto, A. *Biopolymers* **1999**, *50*, 87.
(26) Claire, K.; Pecora, R. *J. Phys. Chem. B* **1997**, *101*, 746.